IEEE Access
Multidisciplinary | Rapid Review | Open Access Journal

Received November 11, 2021, accepted November 28, 2021, date of publication December 10, 2021,
date of current version December 20, 2021.

Digital Object Identifier 10.1109/ACCESS.2021.3134260

Mackerel Fat Content Estimation Using RGB and Depth Images

SHUYA SANO[1], TOMO MIYAZAKI[1], (Member, IEEE), YOSHIHIRO SUGAYA[1], (Member, IEEE), NAOHIRO SEKIGUCHI[2], AND SHINICHIRO OMACHI[1], (Senior Member, IEEE)

[1]Graduate School of Engineering, Tohoku University, Sendai 9808579, Japan
[2]Tohto C-Tech Corporation, Sendai 9830047, Japan

Corresponding author: Tomo Miyazaki (tomo@tohoku.ac.jp)

This work was supported in part by the Japan Society for the Promotion of Science (JSPS) KAKENHI under Grant 20H04201, Grant 19K12033, and Grant 19K11848.

ABSTRACT We propose a method for estimating the fat content of mackerels from their images. The market value of fish varies greatly depending on the fat content. For example, mackerels with high-fat content are a high priority for business transactions in Japanese fisheries. The fat content is commonly measured manually with special equipment using the near-infrared spectroscopy, which increases costs and reduces productivity. It is ideal to estimate the fat content automatically using inexpensive equipment such as ordinary cameras. However, fat content estimation from fish images is a challenging task because the difference in fat content appears only as a slight difference in their appearance. To tackle this problem, we propose to use not only RGB images but also depth images to utilize shape information as well as the textures. To detect subtle differences in texture and shape, we propose a convolutional neural network that extracts and concatenates features from part images, such as the head, body, and tail of a mackerel image. Color-texture and three-dimensional shape features extracted from RGB and depth images, respectively, are combined to estimate the fat content. Experimental results show that the proposed method estimated fat content with 2.25 points at mean absolute error.

INDEX TERMS Fish image analysis, fat content estimation, neural network, RGB image, depth image, fishery industry.

I. INTRODUCTION

The fat content of fish is one of the important factors that determines its market value, and it is important to accurately estimate the fat content. The fat content is now commonly measured manually with special equipment using the near-infrared spectroscopy. However, this method requires additional labor power and special equipment, which increases costs and reduces productivity. A method for automatically estimating the fat content in a non-destructive manner with inexpensive equipment such as ordinary cameras is required. On the other hand, some experts identify high-fat content fish without cutting and checking the cross-section of the fish. They can estimate fat content based on subtle differences in appearance from years of experience. This means that it is not impossible to estimate the fat content from fish images.

In this study, we propose a method for estimating the fat content of fish from their images, targeting mackerels. Mackerel is a popular fish caught in Japan, and its market value varies greatly depending on the fat content. The fat content estimation from fish images is a challenging task because the difference in fat content appears only as a slight difference in their appearance. To tackle this problem, we propose to use not only RGB images but also depth images to utilize shape information as well as the textures. It is known that the body shape of fish changes and the pattern on the body surface also changes by accumulating fat in their body. The shape features from the depth image can improve estimation performance. We also propose to extract features from the head, body, and tail of a mackerel image to detect subtle differences in texture and shape. This feature extraction strategy enables us to focus on local features of texture and shape. Color-texture and three-dimensional shape features extracted from RGB and depth images, respectively, are combined to estimate the fat content.

The associate editor coordinating the review of this manuscript and approving it for publication was Nagarajan Raghavan.

To this end, we propose neural networks to merge these features. Consequently, we can acquire features suitable for fat content estimation.

To show the effectiveness of the proposed method, experiments were conducted to evaluate the accuracy of the estimated fat content. It was shown that the proposed method achieved an absolute error of approximate 2.2 % compared to the values measured by the NIR spectroscopy sensor.

II. RELATED WORKS

A. FISH FAT CONTENT ESTIMATION

The near-infrared (NIR) spectroscopy is a general measurement method for fish fat content in a non-destructive inspection. Almendingen *et al.* used a NIR spectroscopy to determine fat content in homogenized diets [1]. The determined fat content was accurate, and its processing time was more rapid than the traditional technique [2]. Zhang *et al.* applied linear regression to raw data measured by the NIR spectroscopy to determine moisture, protein, and fat content in fish meals [3]. The reported processing time was less than 3 minutes.

Although the NIR spectroscopy is a standard measurement method, it requires a special equipment and additional labor power which increases costs and reduces productivity. It is ideal to estimate the fat content automatically using inexpensive equipment such as ordinary cameras.

B. FISH CLASSIFICATION USING MACHINE LEARNING

It is essential to capture visual patterns in fish images for fish classification. Thus, there are many attempts to exploit machine learning techniques. Fouad *et al.* classified fish images into tilapia and other species [4]. This method used both image processing and machine learning techniques simultaneously. Khotimah *et al.* developed an algorithm for classifying images into three species: bigeye tuna, yellowfin tuna, and skipjack tuna [5]. They used the gray level co-occurrence matrix (GLCC) [6] to extract features from the texture of fish images, and a decision tree was used for classification. Kitasato *et al.* used SVM as a classifier to classify chub mackerel and blue mackerel [7]. They used texture and shape features. The shape feature was measured the dorsal fin's length from the first to the ninth spine in images. Hasija *et al.* developed a method for fish species classification using subspace-based graph matching [8]. Chuang *et al.* classified seven fish species using head size, eye texture, and the tail ratio to the whole body [9]. Hsiao and Chen had developed a fish species classification by matching [10].

Convolutional neural network, CNN, becomes a common approach for fish classification [11]–[15]. Siddiqui *et al.* showed that CNN was effective for fish species classification in an underwater environment, including noise and blur [11]. Ge *et al.* extracted features using CNN and used Gaussian mixture models, GMMs, for fine classification of fish images [12]. Nagaoka *et al.* used CNN to recognize chub and blue mackerels [16]. Also, there are methods based on CNN for classification and detection of other animals [17]–[21]. The results of the methods based on CNN are faster than other methods. Besides, they are robust to noise.

C. REGRESSION ESTIMATION METHODS

Although not concerning fishes, many methods used regression techniques. For example, there are gender and age estimation from face images [22], friction coefficient and hardness estimation of an object [23], and ripeness estimation of a fruit [24]. Most methods used a pre-trained CNN model and trained only layers added to the model [22]–[25]. On the other hand, some methods trained a CNN as a feature extractor and perform regression estimation using decision trees [26], [27]. The methods mentioned used CNNs for feature extraction. The main difference is training CNN from scratch or use of a pre-trained model. Using a pre-trained model, we can train CNN on various datasets since the number of training parameters is limited. Whereas, in the case of training CNNs from scratch, training is not easy because of the large number of parameters.

There is a regression approach by classifying to discrete ranges [22]. The performance of this approach is comparable to the general regression approach. Therefore, we adopt the general regression approach.

III. IMAGE CAPTURE SYSTEM

We illustrate the image capture system in Fig. 1. We capture mackerel images moving on a conveyor belt. The input slope aligns mackerels. We suppose mackerels are isolated, and they should be left direction when they are put on the conveyor belt. We capture RGB image and depth values using an RGB camera and a Time-of-Flight camera (ToF camera), respectively. The distance from the cameras to the conveyor is 480 mm. Illuminance is 8000 lx at the center of the conveyor. The RGB and ToF cameras are Lucid Vision Triton TRI050S-CC and Helios HLS003S-001, respectively. The focal length of the RGB camera is 8 mm. The precision of ToF camera is 0.69 mm. Considering the average thickness 76.5 mm in Table 1, the precision 0.69 mm is sufficient. We performed calibration to obtain pixel-level correspondences between RGB and ToF cameras. We create a depth map by retrieving the depth values corresponding to the RGB image. Consequently, all pixels are matched between the depth map and the RGB image. Also, their sizes are the same, 1024-pixels square. Table 1 shows statistics of four features, length, width, thickness, and weight. Note that we do not use these four features for fat content estimation in this study.

As shown in Fig. 2, we created a pseudo-color image from depth data captured by the ToF camera using the following procedure. We converted the depth data into a gray scale image by

$$g = 1 - \frac{d - D_{\max}}{D_{\max} - D_{\min}}, \tag{1}$$

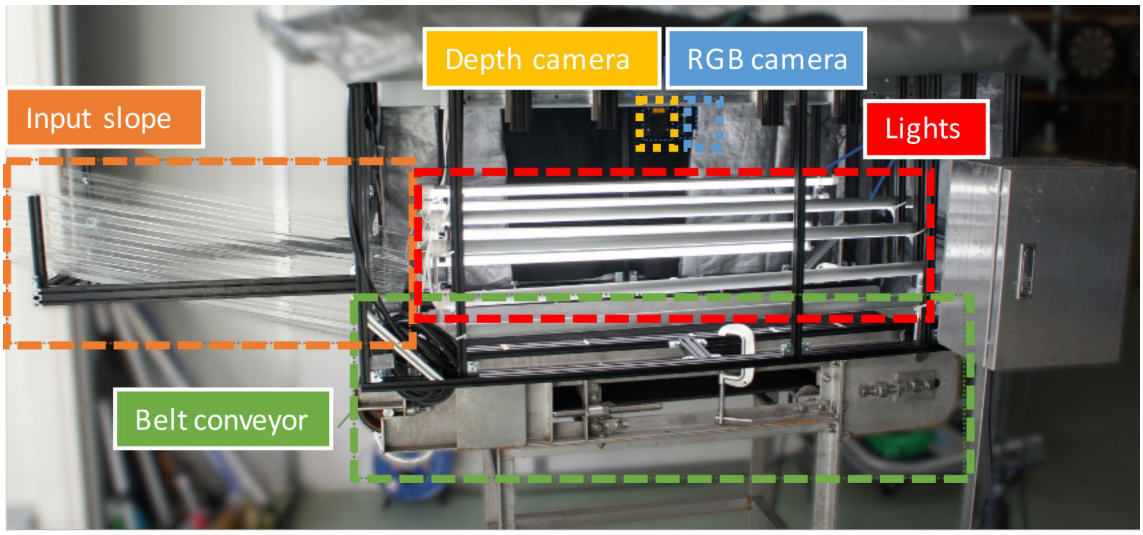

FIGURE 1. The image capture system.

TABLE 1. The statistics of 32 mackerels caught in December 2019.

	Length	Width	Thickness	Weight
Ave	377.6 mm	54.0 mm	76.5 mm	681.5 g
Min	310 mm	39 mm	60 mm	305 g
Max	423 mm	65 mm	89 mm	990 g

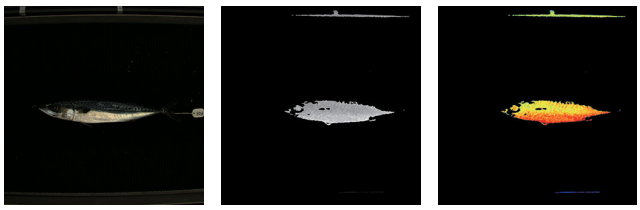

(a) RGB (b) Gray from depth data (c) Pseudo-color image

FIGURE 2. RGB and depth images produced by the system.

where g represents gray scale value, d is measured depth. $D_{\max}$ and $D_{\min}$ are maximum and minimum depth values, respectively. In this study, we set $D_{\max}$ as 535 (mm), $D_{\min}$ as 420 (mm). The thick regions in the converted gray scale image will be bright. Then, we assigned zero to missing values in the depth data. Subsequently, we apply a median filter with 3×3 kernel size to the gray image to remove noise in the gray image since the conveyor belt absorbs infrared radiation from the ToF camera. Finally, we converted the gray image into a pseudo-color image using a jet color map. Hereafter, the depth image denotes the pseudo-color image, which is input to the neural networks. Since it is difficult to extract the shape information from the RGB image, the depth image complements the RGB image. We resize the original image size, 1024 pixels square, to 224 pixels square since we adopt the VGG16 model [28] in this study.

The RGB image contains information such as the color and texture of the mackerel. On the other hand, the depth image has the three-dimensional shape information of the mackerel. Therefore, RGB and depth images play complementary roles.

IV. FAT CONTENT ESTIMATION

We show the overview of the proposed fat content estimation algorithm in Fig. 3. The proposed method is composed of three modules. The first module estimates the mackerel region in the input image. The second module generates global and local images of the mackerel using the estimated region. Finally, the third module estimates the fat content using the global and the local images.

A. MACKEREL REGION ESTIMATION

The only object in the input image should be a mackerel. However, some parts of the image capture system, such as the conveyor belt, exists in the image. To crop only the mackerel image as accurately as possible, we estimate the mackerel region accurately in the image.

In this study, we utilize the VGG16 model [28] for the region estimation, which is trained on ImageNet [29] to capture 1000 classes of objects in various situations. A wide range of applications uses the VGG 16 model since it can extract features from objects with various shapes and colors. Moreover, the model can fit various datasets, even a small one. The model contains 13 convolutional layers, and each convolutional layer extracts high dimensional features by increasing the number of channels while decreasing the image size. Specifically, we use the first layer's feature map to maintain the mackerel's resolution. This feature map activates the locations of the object. As shown in Fig. 4 (a), the feature map focuses strongly on mackerel. Therefore, we can accurately estimate the mackerel region in the image using the feature map.

We describe details of the algorithm for mackerel region estimation. We experimentally set the thresholds and other parameters.

1) *Feature Map Extraction:* We extract a feature map from the RGB image using the first layer of the VGG16 model. Subsequently, we reduce the number

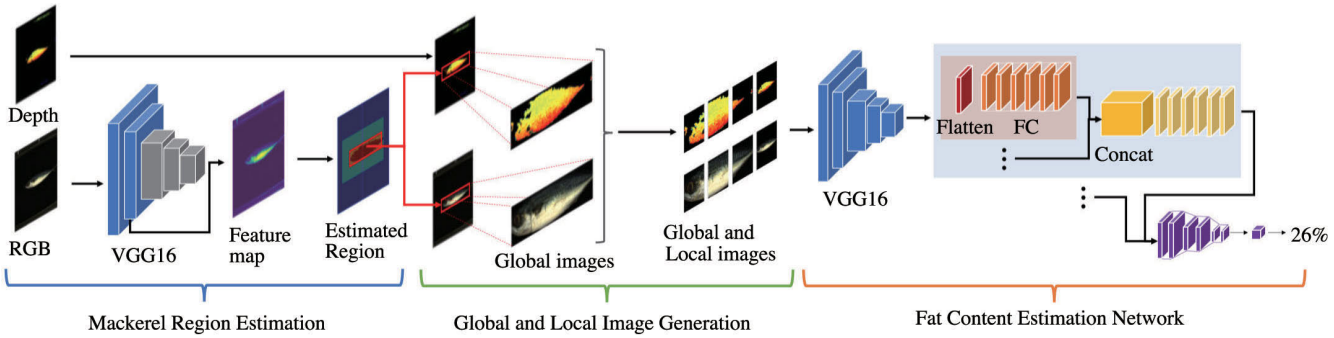

FIGURE 3. The overview of the proposed method.

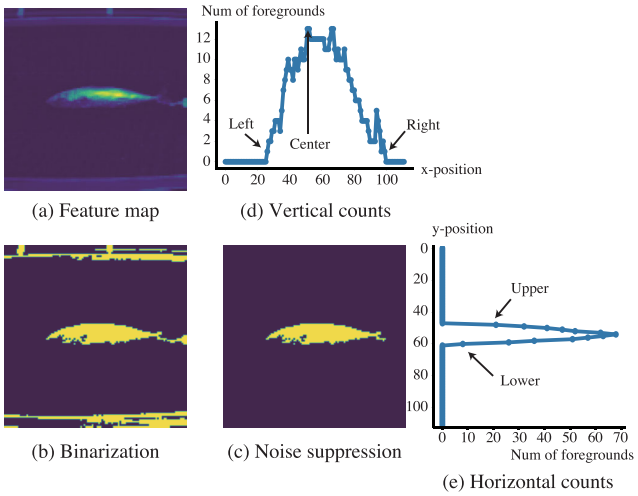

FIGURE 4. The output examples of the mackerel region estimation.

of channels of the feature map 64 to 1 by taking max in the channels. Fig. 4 (a) shows an example.

2) *Binarization:* We binarize the feature map using a threshold 9. The values in foreground and background become 1 and 0, respectively. An example is in Fig. 4 (b).
3) *Noise Suppression:* We suppress the outer area of the predefined region by making the values to 0. The predefined region is a box with left-top (10, 30), width 90, and height 50. An example is shown in Fig. 4 (c).
4) *Left and Right Position Search:* As shown in Fig. 4 (d), we count foreground pixels vertically. The left position is the first non-zero pixel from the most left. Likewise, the right position is the last pixel.
5) *Upper and Lower Position Search:* As shown in Fig. 4 (e), we count foreground pixels horizontally. The upper position is the first non-zero pixel from the most top. Likewise, the lower position is the last pixel.

B. GLOBAL AND LOCAL MACKEREL IMAGE GENERATION

We generate global and local images of the mackerel. As shown in Fig. 5, we define the global image as the whole

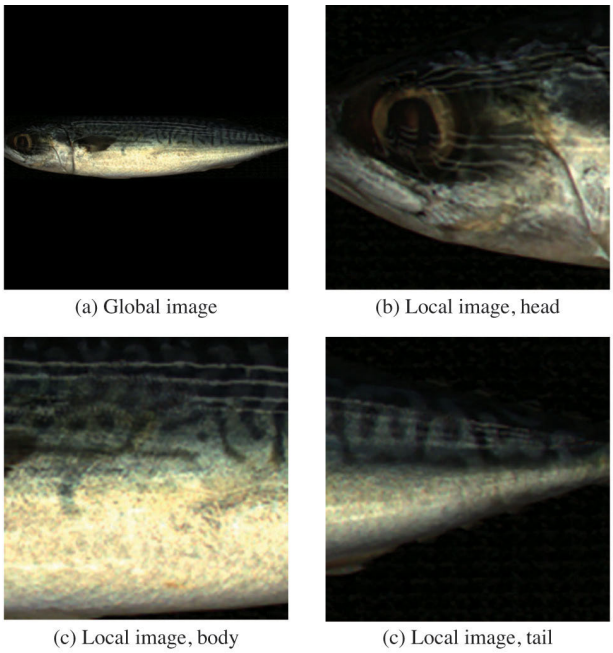

FIGURE 5. Global and local images.

mackerel part. The local images are the head, body, and tail of the mackerel.

We produce the global image by cropping the estimated region. We resize the cropped image to 224-pixel square by adding margins. The VGG16 model is trained on 224-pixel square images. To take advantage of the performance of the trained VGG16, we adopt the same image size. The global image contains texture and shape features of the mackerel. However, local information may lose due to the low resolution caused by resizing.

We create local images of the mackerel's parts, such as the head, body, and tail, to maintain the resolution of the details. We crop h-pixel squares from the estimated region, where h is the height of the estimated region. Precisely, we extract body square so that its center is the first position that maximizes the vertical count of foreground pixels as shown in Fig. 4 (d). The head and tail squares are adjacent to the body square. Finally, we resize the h-pixel squares to 224-pixel squares. We can extract features from the local

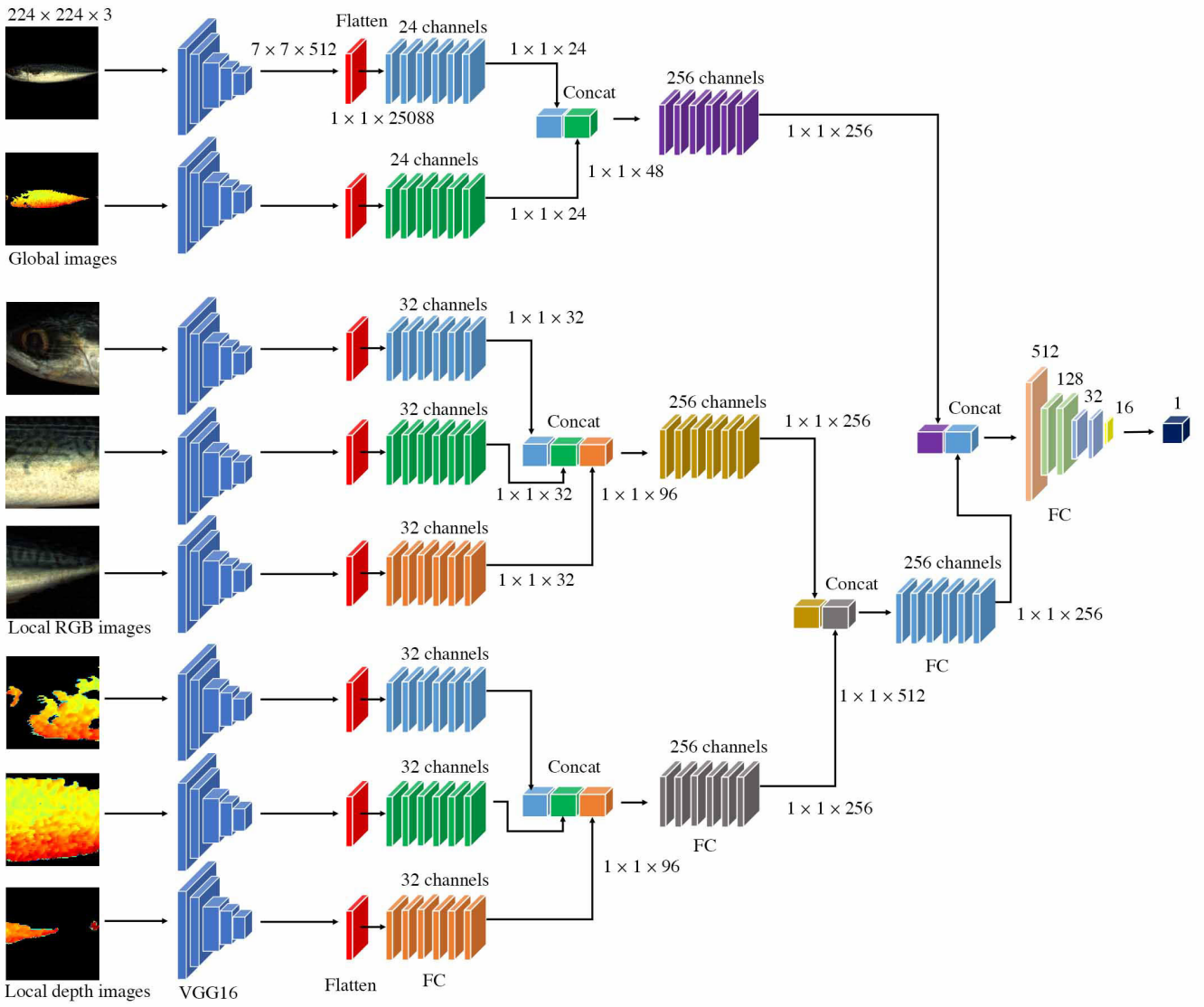

FIGURE 6. Fat content estimation network.

images that complement features from the global image. Also, we produce depth global and local images using the locations of the RGB local images.

C. FAT CONTENT ESTIMATION NETWORK

We use neural networks to estimate fat content from the global and local images of RGB and Depth. We show the configuration of the network in Fig. 6. We apply the VGG16 model without the fully connected layers to all the input images to extract feature maps, resulting in feature matrices $\mathbb{R}^{7\times7\times512}$. Every fully connected layer has one hidden layer. We use the VGG16 model as a feature extractor to extract texture features instead of using hand-crafted texture features, such as LTP [30] and LQP [31]. Then, we gradually merge features and produce the final feature to estimate fat content. Specifically, we use flatten layer to transform the feature matrices into one-dimensional vector $\mathbb{R}^{1\times25088}$. We apply six fully connected layers that produce feature matrices $\mathbb{R}^{1\times1\times24}$ and $\mathbb{R}^{1\times1\times32}$ for global and local images, respectively. Then, we merge and produce features using concatenation and fully connected layers. The VGG16 is the configuration D model trained on ImageNet.

1) IMPORTANCE FOR SAMPLES

The fat content is biased in the dataset. There are only few samples of extremely low- and high-fat content. They are the minority. A simple training tends to learn the fat contents that are majorities in the dataset. However, it is difficult to learn the fat contents of minorities, such as extremely low- and high-fat content. To solve this problem, we assign importance to each sample to learn all samples' fat content. Specifically, we assign high importance to minority samples and train them with a high learning rate to encourage the networks to learn the minorities. On the other hand, the majority samples

are assigned with low importance to suppress learning them. Consequently, we can mitigate the bias of the dataset and prevent overtraining.

We calculate importance W_i for sample i by (2). Specifically, we normalized the fat content to [0.0, 1.0] and created a histogram of fat content from the dataset.[1] Then, we divide the bin value m_i by the maximum value $m_{\max}$ of all bins.

$$W_i = \left(\frac{m_i}{m_{\max}}\right)^{-1} = \frac{m_{\max}}{m_i} \tag{2}$$

2) NORMALIZATION

To facilitate training, we normalize the fat content to [0, 1]. We define the normalization used in this study as Eq. (3). We obtain the maximum $E_{\max}$ and minimum $E_{\min}$ from training data when we normalize fat content. We use the maximum value $E_{\max}$ in the training data to normalize RGB and depth images as defined in Eq. (4).

$$y_{\text{norm}} = \frac{y - E_{\min}}{E_{\max} - E_{\min}} \tag{3}$$

$$x_{\text{norm}} = \frac{x}{E_{\max}} \tag{4}$$

D. IMPLEMENTATION DETAILS

As we described, the feature extractor is the VGG16 model trained on ImageNet. We freeze the parameters of the VGG16 model. Thus, we use the fixed parameters to extract features during training and test. The number of parameters in the entire estimation network is 21,407,585, while, the number of training parameters is 13,772,321. We describe the hyperparameters used in this study below. The batch size is 32, the number of epochs is 100, the loss function is mean squared error (MSE), the optimization algorithm is SGD (stochastic gradient descent optimizer), the learning rate is 2.5×10^{-3}, and the momentum is 0.9. Also, we used 20% of the training data as validation data. We determine the best model using the validation data over the epochs. Tensorflow 1.9.0, a framework for machine learning, was used for the implementation, and the official Tensorflow Docker image file[2] was used to build the environment. We use Intel i7-6850K CPU, 128 GB RAM, and GeForce GTX1080Ti GPU.

V. EXPERIMENTS

We show the dataset's specification in the experiments in Table 2. The number of mackerels used in the dataset was 287, with a minimum and maximum fat contents of 10.53% and 33.17%, respectively. To ensure that the training and test datasets are independent, we used the images taken in October 2019 for training data, and the test data are taken in February 2020.

We measured ground truth of mackerel fat content using a NIR spectroscopy sensor, NIR-GUN.[3] We put the NIR spectroscopy sensor to a position where a few millimeters from the anus to the tail. The abdomen of a mackerel accumulates fats in a short time. On the other hand, the anus needs a long time to accumulate fat since there are no organs on the tail side of the anus. Therefore, the measurement of the anus is more stable than that of the abdomen.

TABLE 2. Statistics in dataset.

	Images	Fat Ave	Fat var	Fat std
Train	2541	19.59	26.35	5.13
Test	2016	19.12	27.32	5.22

We used four evaluation criteria: mean absolute error (MAE), root mean square error (RMSE), R2-score, and correlation coefficient. We describe each criterion using ground truth y, estimated value y', and the mean of all ground truth $\bar{y}$. The MAE is defined as (5). MAE averages error between the y and y', where the smaller the error, the more accurate the estimation. RMSE is defined as (6). RMSE considers large errors as more important. Compared to the MAE, RMSE is sensitive to outliers with large gaps between ground truth and estimated values. R2-score in (7) is ranging from zero and one. The closer to one, the performance is better. The correlation coefficient evaluates the correlation between the estimated values and the ground truth. The correlation coefficient is equal to the root of R2-score.

$$\text{MAE} = \frac{1}{n}\sum_i |y_i - y'_i| \tag{5}$$

$$\text{RMSE} = \sqrt{\frac{1}{n}\sum_i (y_i - y'_i)^2} \tag{6}$$

$$\text{R2} = 1 - \frac{\sum_i (y_i - y'_i)^2}{\sum_j (y_j - \bar{y})^2} \tag{7}$$

A. RESULT ON FAT CONTENT ESTIMATION

We compared the proposed model to typical regression and deep learning models. We used VGG16 and VGG19 as the deep learning models, which are regarded as baselines. We replace the existing fully connected layers of the VGG16 and VGG19 with a new fully connected layer. The input for the baselines is an RGB image obtained by the image capture system, which is shown in Fig. 2. We trained only the replaced fully connected layer.

The typical regression models are Support Vector Regression (SVR) [32], random forest (RF), and gradient boosting (GB) [33], [34]. We extracted feature vectors from 224-pixel square images using Histogram of Oriented Gradients (HOG) descriptor [35]. The dimension of a HOG descriptor is 54756. We used radial basis function kernel in SVR. The random forest and gradient boosting models used ten weak classifiers.

We illustrated the evaluation results using the proposed method in Table 3. The baselines and the proposed method obtained more than 0.7 points at correlation coefficient and less than 3.0 points at MAE. Furthermore, the proposed method outperformed the baselines in all the evaluation criteria. In particular, the RMSE of the proposed method was less than 3, whereas the RMSE of the baselines was more

[1] We experimentally set bin width to 0.01.

[2] tensorflow/tensorflow:1.9.0-gpu-py3

[3] FQA-NIR GUN (Food Quality Analyzer) by FANTEC Co., Ltd.

TABLE 3. Results on fat content estimation.

	MAE	RMSE	R2	Correlation
Gradient boosting	4.16	4.89	0.13	0.43
SVR	3.82	4.73	0.18	0.45
Random forest	3.81	4.65	0.21	0.46
VGG16	2.54	3.38	0.58	0.77
VGG19	2.50	3.3	0.61	0.79
Proposed	**2.25**	**2.91**	**0.69**	**0.83**

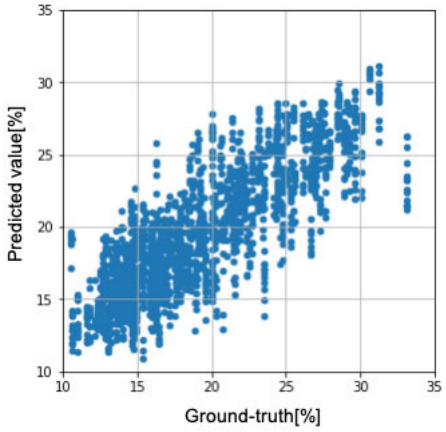

FIGURE 7. Scatter plots of the estimated fat content.

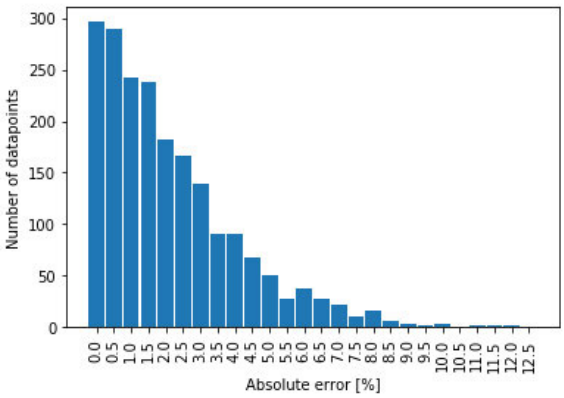

FIGURE 8. Histogram of the errors in the estimated fat content.

than 3.2. The results indicate the effectiveness of the proposed method.

We showed a scatter plot of the evaluation results in Fig. 7. Also, Fig. 8 shows a histogram of the errors. The maximum error was 12%. The number of test samples in less than 4% error was about 1700, which is more than 84 % of the test samples.

We investigated the effect of epochs. Specifically, we train the proposed model using epoch 500. Then, we evaluated the models at a 50 epoch period. As shown in Fig. 9, the losses converged until epoch 50. The mean absolute errors were comparable after epoch 50. Therefore, epoch 100 is sufficient.

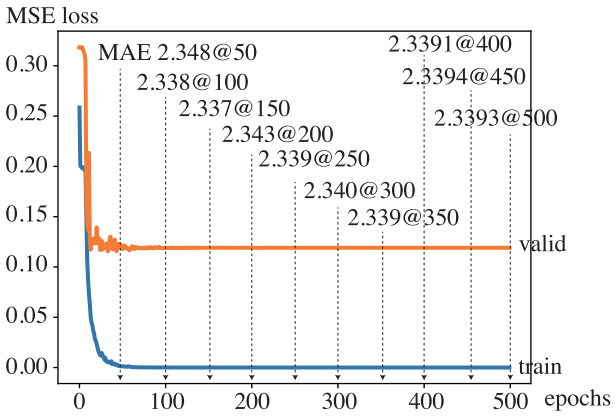

FIGURE 9. MSE loss curves and MAE on test data in epochs.

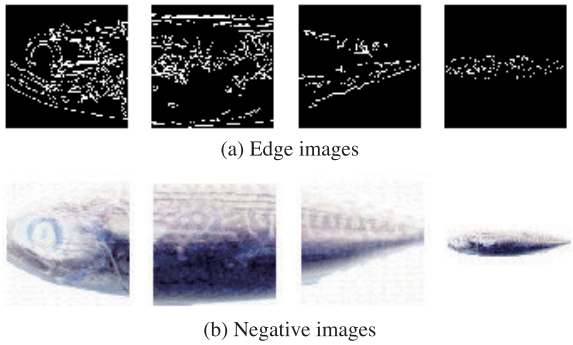

FIGURE 10. Replacements for the depth images.

The average processing time was 33 ms per image over the test dataset by the proposed method. Most parts of the processing time were required by the VGG model. The two modules took 5.8 ms and 27.2 ms for the mackerel region estimation and the fat content estimation network, respectively. It took 0.02 ms by the global and local image generation.

B. COMPARISON ON FEATURE EXTRACTORS

The proposed method uses the VGG16 model as a feature extraction CNN. The VGG16 plays a vital role in range estimation in the proposed method. However, there are various CNN models other than the VGG16. We carried out experiments using other models as feature extractors to search for a better feature extractor.

We used Xception [36], Inceptionv3 [37], Resnet50 [38], and DenseNet [39]. The evaluation results using ResNet50 are 6.8057 at MAE and 0.078625 at the correlation coefficient. However, the learning processes of these models were not converged. The fail of training may be due to the large number of parameters to be trained. The dataset is insufficient to train them. We note that the same phenomenon has reported in [24]. Besides, the consumption of hardware resources and the computation time increased. Specifically, it costs 45.5 (ms/image) on VGG16, whereas 140 (ms/image) on ResNet50. Therefore, VGG16 is considered to be more practical for our system.

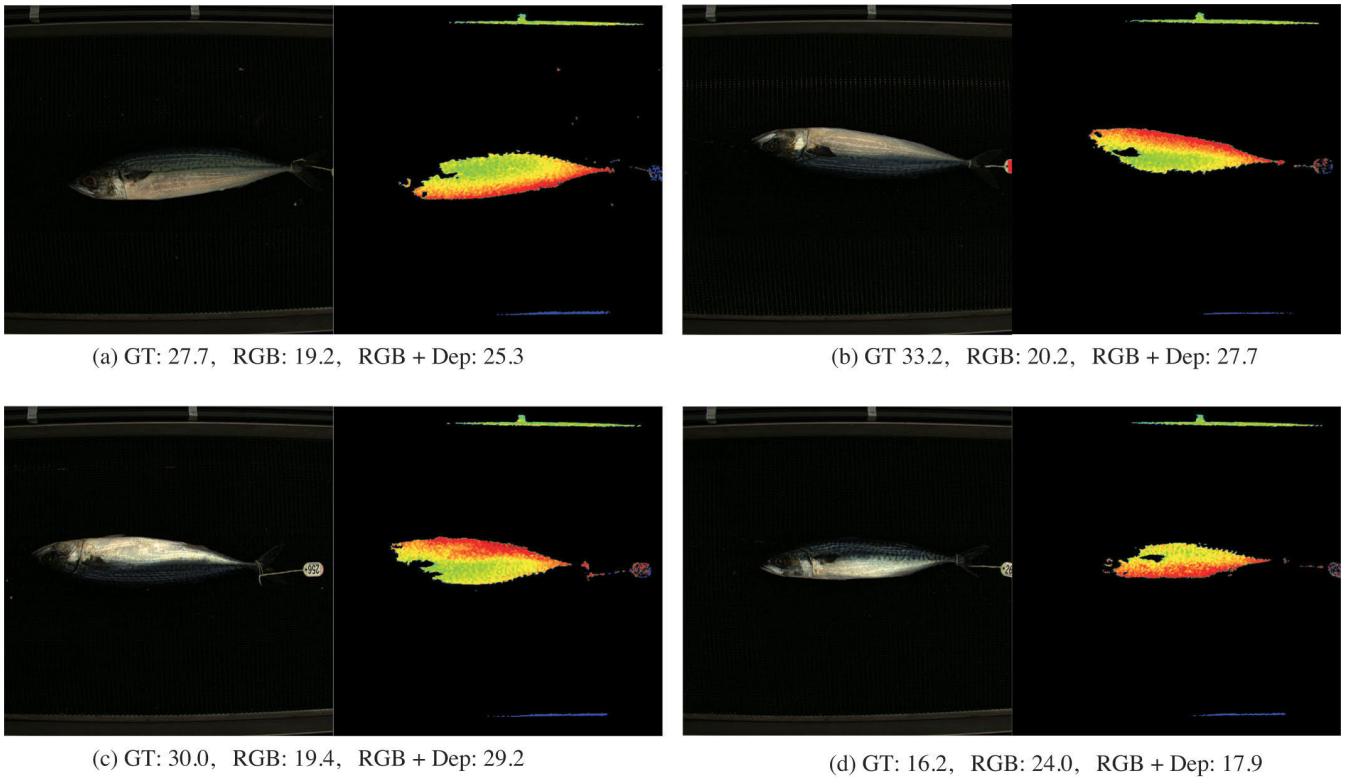

(a) GT: 27.7, RGB: 19.2, RGB + Dep: 25.3

(b) GT 33.2, RGB: 20.2, RGB + Dep: 27.7

(c) GT: 30.0, RGB: 19.4, RGB + Dep: 29.2

(d) GT: 16.2, RGB: 24.0, RGB + Dep: 17.9

FIGURE 11. Estimated fat content w/wo depth image.

TABLE 4. Results with or without the local images.

	MAE	RMSE	R2	Correlation
Without	2.39	3.13	0.64	0.80
With	2.25	2.91	0.69	0.83

C. VERIFICATION ON LOCAL IMAGES

To verify the effectiveness of using the local images, we compared the proposed method with and without the RGB and depth local images. We showed the experimental results in Table 4. The performance improved with the local images. Therefore, we confirmed that the local images contributed to the fat content estimation. Mackerels store fat in their skin to keep the body temperature. Thus, the skin textures extracted by VGG16 from RGB images are essential to estimate fat content. According to the results, the local images captured the texture. We successfully extract features from the local images for fat content estimation.

D. VERIFICATION ON DEPTH IMAGES

We carried out the experiments to verify the effectiveness of the depth image. We evaluated the proposed method by removing the depth images and the related layers. Also, we replaced the depth images with negative images and edge images. Fig. 10 shows examples of the replaced images.

The experimental results are shown in Table 5. In all cases, the depth image marked the best accuracy. The results confirmed the significance of the depth image. We show the estimated fat content with and without depth image in Fig. 11. The results demonstrated the effectiveness of the feature extraction from depth images.

TABLE 5. Results for depth image removal and replacements.

	MAE	RMSE	R2	Correlation
Without depth	2.39	3.15	0.64	0.80
Negative	2.51	3.32	0.60	0.60
Edge	2.55	3.32	0.60	0.78
With Depth	2.25	2.91	0.69	0.83

E. DISCUSSION ON THE LENGTH OF MACKERELS

We discuss the effect of the length of mackerels on fat content estimation. The proposed method cropped mackerels and resized them into the fixed size, 224×224. Therefore, the proposed method omitted the actual length of the mackerels. We analyzed the relationships between length and fat content. The results are shown in Fig. 12. We used the 32 mackerels caught in December 2019, which are the same as Table 1. We obtained the approximate line $y = 0.127x - 31.05$ using the least square method. The results show that there is a correlation between length and fat content. Therefore, we can expect further improvements by incorporating length information into the fat content estimation.

F. DISCUSSION ON FISH DIRECTION

We investigated the directions of fishes in the dataset. The up and down directions are 47% and 53% in the training data, 43% and 57% in the test data. All fishes have left direction. For evaluation of fish direction, we conducted

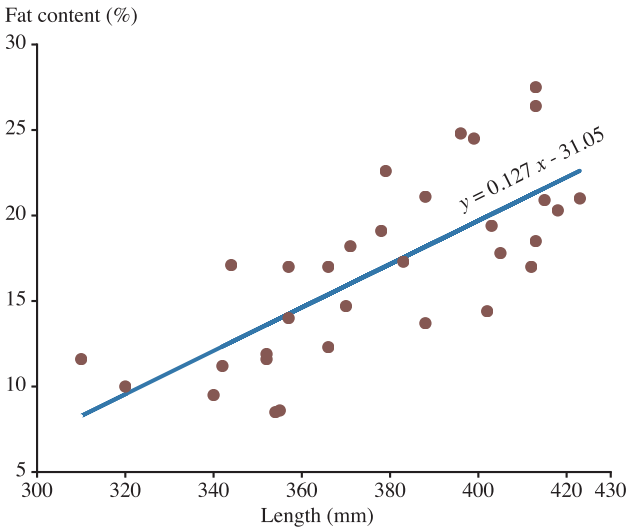

FIGURE 12. The scatter plot of length and fat content.

TABLE 6. Mean absolute error with and without data augmentation.

training data		test data		
Vertical	Horizontal	Original	Vertical	Horizontal
-	-	2.25	2.74	3.18
✓	-	2.13	2.34	3.12
-	✓	2.04	2.58	2.24
✓	✓	1.67	1.71	2.01

experiments using vertical and horizontal flips. Specifically, we trained models using data augmentation with vertical and horizontal flips to the training data. Then, we evaluated the trained models on the test data using the flips. Table 6 shows that the model trained with the original training data was suffered from the flipped test data. The performance improved using data augmentation on all test data. Therefore, data augmentation with the flips is effective for fat content estimation.

VI. CONCLUSION

We proposed a method for estimating the fat content of mackerels from RGB and depth images. The proposed method estimates the mackerel region with a small computational cost using the feature map of the VGG16 model. The global and local images that contain the whole mackerel, head, body, and tail are extracted from the estimated region, and the features are extracted from the global and local images of RGB and depth. The extracted features are merged gradually and the fat content of the mackerel is estimated.

We conducted experiments to compare the estimated fat content with the values measured by the NIR spectroscopy sensor. The experimental results show the effectiveness of the proposed method. Introducing the proposed system to the fish market and assessing the effectiveness of the proposed method in a real situation is an important future work. In this study, we conducted experiments on mackerel, however, the proposed method can be used for other fish as well. It is also a future work to confirm the effectiveness of the proposed method for various kinds of fish.

REFERENCES

[1] K. Almendingen, H. Meltzer, J. Pedersen, B. Nilsen, and M. Ellekjær, "Near infrared spectroscopy—A potentially useful method for rapid determination of fat and protein content in homogenized diets," *Eur. J. Clin. Nutrition*, vol. 54, no. 1, pp. 20–23, Jan. 2000.

[2] B. Borgström, R. Nordèn, B. Åkesson, and M. Jägerstad, "A study of the food consumption by the duplicate portion technique in a sample of the Dalby population," *Scand. J. Social Med.*, vol. 10, pp. 9–98, Jan. 1975.

[3] H.-Z. Zhang, W. Zeng, M. Rutman, and T.-C. Lee, "Simultaneous determination of moisture, protein and fat in fish meal using near-infrared spectroscopy," *Food Sci. Technol. Res.*, vol. 6, no. 1, pp. 19–23, 2000.

[4] M. M. M. Fouad, H. M. Zawbaa, N. El-Bendary, and A. E. Hassanien, "Automatic Nile Tilapia fish classification approach using machine learning techniques," in *Proc. 13th Int. Conf. Hybrid Intell. Syst. (HIS)*, Dec. 2013, pp. 173–178.

[5] W. N. Khotimah, A. Z. Arifin, A. Yuniarti, A. Y. Wijaya, D. A. Navastara, and M. A. Kalbuadi, "Tuna fish classification using decision tree algorithm and image processing method," in *Proc. Int. Conf. Comput., Control, Informat. Appl. (IC3INA)*, Oct. 2015, pp. 126–131.

[6] P. Mohanaiah, P. Sathyanarayana, and L. GuruKumar, "Image texture feature extraction using GLCM approach," *Int. J. Sci. Res. Publications*, vol. 3, no. 5, p. 1, 2013.

[7] A. Kitasato, T. Miyazaki, Y. Sugaya, and S. Omachi, "Automatic discrimination between *Scomber japonicus* and *Scomber australasicus* by geometric and texture features," *Fishes*, vol. 3, no. 3, no. 3, p. 26, Sep. 2018.

[8] S. Hasija, M. J. Buragohain, and S. Indu, "Fish species classification using graph embedding discriminant analysis," in *Proc. Int. Conf. Mach. Vis. Inf. Technol. (CMVIT)*, 2017, pp. 81–86.

[9] M.-C. Chuang, J.-N. Hwang, F.-F. Kuo, M.-K. Shan, and K. Williams, "Recognizing live fish species by hierarchical partial classification based on the exponential benefit," in *Proc. IEEE Int. Conf. Image Process. (ICIP)*, Oct. 2014, pp. 5232–5236.

[10] Y.-H. Hsiao and C.-C. Chen, "Over-atoms accumulation orthogonal matching pursuit reconstruction algorithm for fish recognition and identification," in *Proc. 23rd Int. Conf. Pattern Recognit. (ICPR)*, Dec. 2016, pp. 1071–1076.

[11] S. A. Siddiqui, A. Salman, M. I. Malik, F. Shafait, A. Mian, M. R. Shortis, and E. S. Harvey, "Automatic fish species classification in underwater videos: Exploiting pre-trained deep neural network models to compensate for limited labelled data," *ICES J. Mar. Sci.*, vol. 75, no. 1, pp. 374–389, 2017.

[12] Z. Ge, C. McCool, C. Sanderson, and P. Corke, "Modelling local deep convolutional neural network features to improve fine-grained image classification," in *Proc. IEEE Int. Conf. Image Process. (ICIP)*, Sep. 2015, pp. 4112–4116.

[13] G. Ding, Y. Song, J. Guo, C. Feng, G. Li, B. He, and T. Yan, "Fish recognition using convolutional neural network," in *Proc. OCEANS, Anchorage*, 2017, pp. 1–4.

[14] D. Rathi, S. Jain, and D. S. Indu, "Underwater fish species classification using convolutional neural network and deep learning," 2018, *arXiv:1805.10106*.

[15] L. Meng, T. Hirayama, and S. Oyanagi, "Underwater-drone with panoramic camera for automatic fish recognition based on deep learning," *IEEE Access*, vol. 6, pp. 17880–17886, 2018.

[16] Y. Nagaoka, T. Miyazaki, Y. Sugaya, and S. Omachi, "Automatic mackerel sorting machine using global and local features," *IEEE Access*, vol. 7, pp. 63767–63777, 2019.

[17] W. Xu and S. Matzner, "Underwater fish detection using deep learning for water power applications," 2018, *arXiv:1811.01494*.

[18] S. Choi, "Fish identification in underwater video with deep convolutional neural network: SNUMedinfo at LifeCLEF fish task 2015," in *Proc. CLEF, Working Notes*, 2015, pp. 1–5.

[19] X. Li, M. Shang, H. Qin, and L. Chen, "Fast accurate fish detection and recognition of underwater images with fast R-CNN," in *Proc. OCEANS, MTS/IEEE Washington*, Oct. 2015, pp. 1–5.

[20] R. Mandal, R. M. Connolly, T. A. Schlacher, and B. Stantic, "Assessing fish abundance from underwater video using deep neural networks," in *Proc. Int. Joint Conf. Neural Netw. (IJCNN)*, Jul. 2018, pp. 1–6.

[21] D. Zhang, G. Kopanas, C. Desai, S. Chai, and M. Piacentino, "Unsupervised underwater fish detection fusing flow and objectiveness," in *Proc. IEEE Winter Appl. Comput. Vis. Workshops (WACVW)*, Mar. 2016, pp. 1–7.

[22] K. Ito, H. Kawai, T. Okano, and T. Aoki, "Age and gender prediction from face images using convolutional neural network," in *Proc. Asia–Pacific Signal Inf. Process. Assoc. Annu. Summit Conf. (APSIPA ASC)*, Nov. 2018, pp. 7–11.
[23] Y. Mikawa, Y. Makino, and H. Shinoda, "Softness estimation based on images of pushing action using deep learning," *Trans. Virtual Reality Soc. Jpn.*, vol. 23, no. 4, pp. 239–248, 2018.
[24] S. Tatemoto, Y. Harada, and K. Imai, "Image-based determination of plum 'Tsuyuakane' ripeness via deep learning," *Agricult. Inf. Res.*, vol. 28, no. 3, pp. 108–114, 2019.
[25] Z. Niu, M. Zhou, L. Wang, X. Gao, and G. Hua, "Ordinal regression with multiple output CNN for age estimation," in *Proc. IEEE Conf. Comput. Vis. Pattern Recognit. (CVPR)*, Jun. 2016, pp. 4920–4928.
[26] W. Li, J. Lu, J. Feng, C. Xu, J. Zhou, and Q. Tian, "BridgeNet: A continuity-aware probabilistic network for age estimation," in *Proc. IEEE/CVF Conf. Comput. Vis. Pattern Recognit. (CVPR)*, Jun. 2019, pp. 1145–1154.
[27] E. Frank and M. Hall, "A simple approach to ordinal classification," in *Machine Learning: ECML 2001*. Berlin, Germany: Springer, 2001, pp. 145–156.
[28] K. Simonyan and A. Zisserman, "Very deep convolutional networks for large-scale image recognition," in *Proc. Int. Conf. Learn. Represent.*, 2015, pp. 1–14.
[29] O. Russakovsky, J. Deng, H. Su, J. Krause, S. Satheesh, S. Ma, Z. Huang, A. Karpathy, A. Khosla, M. Bernstein, A. C. Berg, and L. Fei-Fei, "ImageNet large scale visual recognition challenge," *Int. J. Comput. Vis.*, vol. 115, no. 3, pp. 211–252, 2015.
[30] S. Fekri-Ershad, "Bark texture classification using improved local ternary patterns and multilayer neural network," *Expert Syst. Appl.*, vol. 158, Nov. 2020, Art. no. 113509.
[31] L. Armi and S. Fekri-Ershad, "Texture image classification based on improved local quinary patterns," *Multimedia Tools Appl.*, vol. 78, no. 14, pp. 18995–19018, 2019.
[32] C.-C. Chang and C.-J. Lin, "LIBSVM: A library for support vector machines," *ACM Trans. Intell. Syst. Technol.*, vol. 2, no. 3, pp. 1–27, Apr. 2011.
[33] J. H. Friedman, "Greedy function approximation: A gradient boosting machine," *Ann. Statist.*, vol. 29, no. 5, pp. 1189–1232, Oct. 2001. [Online]. Available: http://www.jstor.org/stable/2699986
[34] A. Alsahaf, G. Azzopardi, B. Ducro, E. Hanenberg, R. F. Veerkamp, and N. Petkov, "Estimation of muscle scores of live pigs using a kinect camera," *IEEE Access*, vol. 7, pp. 52238–52245, 2019.
[35] N. Dalal and B. Triggs, "Histograms of oriented gradients for human detection," in *Proc. IEEE Comput. Soc. Conf. Comput. Vis. Pattern Recognit. (CVPR)*, vol. 1, Jun. 2005, pp. 886–893.
[36] F. Chollet, "Xception: Deep learning with depthwise separable convolutions," in *Proc. IEEE Conf. Comput. Vis. Pattern Recognit. (CVPR)*, Jul. 2017, pp. 1800–1807.
[37] C. Szegedy, V. Vanhoucke, S. Ioffe, J. Shlens, and Z. Wojna, "Rethinking the inception architecture for computer vision," in *Proc. IEEE Conf. Comput. Vis. Pattern Recognit. (CVPR)*, Jun. 2016, pp. 2818–2826.
[38] K. He, X. Zhang, S. Ren, and J. Sun, "Deep residual learning for image recognition," in *Proc. IEEE Conf. Comput. Vis. Pattern Recognit. (CVPR)*, Jun. 2016, pp. 770–778.
[39] G. Huang, Z. Liu, L. Van Der Maaten, and K. Q. Weinberger, "Densely connected convolutional networks," in *Proc. IEEE Conf. Comput. Vis. Pattern Recognit. (CVPR)*, Jul. 2017, pp. 2261–2269.

SHUYA SANO received the B.E. degree from the Division of Information and Electronic System Engineering, Advanced Engineering Course, National Institute of Technology Sendai College, in 2016, and the M.E. degree from the Graduate School of Engineering, Tohoku University, in 2021. He joined Yamaha Motor Company Ltd., in 2016, and has worked as an Engineer at Tohoku University, from 2017 to 2018. He currently works at FANUC CORPORATION as a Software Engineer. His research interest includes image processing using deep neural networks.

TOMO MIYAZAKI (Member, IEEE) received the B.E. degree from the Department of Informatics, Faculty of Engineering, Yamagata University, in 2006, and the M.E. and Ph.D. degrees from the Graduate School of Engineering, Tohoku University, in 2008 and 2011, respectively. He joined Hitachi, Ltd., in 2011, and has worked as a Researcher at the Graduate School of Engineering, Tohoku University, from 2013 to 2014. Since 2015, he has been an Assistant Professor. His research interests include pattern recognition and image processing. He is a member of the Institute of Electronics, Information and Communication Engineers.

YOSHIHIRO SUGAYA (Member, IEEE) received the B.E., M.E., and Ph.D. degrees from Tohoku University, Sendai, Japan, in 1995, 1997, and 2002, respectively. He is currently an Associate Professor at the Graduate School of Engineering, Tohoku University. His research interests include the areas of computer vision, pattern recognition, image processing, and parallel processing and distributed computing. He is a member of the Institute of Electronics, Information and Communication Engineers (IEICE) and the Information Processing Society of Japan.

NAOHIRO SEKIGUCHI received the B.E. and M.E. degrees from The University of Electro-Communications, in 1996 and 1998, respectively. He is currently a Technology Analyst at Tohto C-Tech Corporation, Japan. His research interests include computer vision, robotics, and machine learning.

SHINICHIRO OMACHI (Senior Member, IEEE) received the B.E., M.E., and Ph.D. degrees in information engineering from Tohoku University, Japan, in 1988, 1990, and 1993, respectively. He worked as a Research Associate at the Education Center for Information Processing, Tohoku University, from 1993 to 1996. Since 1996, he has been with the Graduate School of Engineering, Tohoku University, where he is currently a Professor. From 2000 to 2001, he was a Visiting Associate Professor at Brown University. His research interests include pattern recognition, computer vision, image processing, image coding, and parallel processing. He is a member of the Institute of Electronics, Information and Communication Engineers and among others. He received the IAPR/ICDAR Best Paper Award, in 2007, the Best Paper Method Award of the 33rd Annual Conference of the GfKl, in 2010, the ICFHR Best Paper Award, in 2010, and the IEICE Best Paper Award, in 2012.